XUV-laser spectrometer for direct absorption measurements: application to CO in the wavelength range 95−97 nm

P. C. Hinnen, S. Stolte, W. Hogervorst, and W. Ubachs

Laser Centre, Vrije Universiteit, De Boelelaan 1081-1083, 1081 HV Amsterdam, The Netherlands

A narrowband and tunable XUV-laser source, based on harmonic generation of visible laser light, is developed for sensitive and direct absorption measurements. A novel method to monitor and eliminate the fluctuating intensity of this source is developed, which increases the sensitivity for absorption by an order of magnitude. This procedure allows for accurate relative cross-section measurements, demonstrated on selected bands of CO in the wavelength range 95–97 nm.   © 1998 Optical Society of America [S0740-3224(98)00510-4]

OCIS codes: 020.4900, 140.7240, 300.1030, 300.6540.

1. INTRODUCTION

Since the pioneering work of Lyman at the beginning of this century, various light sources have been developed for the extreme-ultraviolet (XUV) spectral region, defined here as the domain where the wavelength $\lambda <$ 105 nm. This value corresponds to the lithium-fluoride cutoff, below which no transparent window materials exist. Nowadays, in addition to classical glow discharges, synchrotron sources are powerful instruments to measure cross sections at short wavelengths,[1] but with a moderate capability to absolutely calibrate spectral data. Recently sources based on the generation of harmonics of tunable pulsed lasers have become available. Tunable and narrowband XUV-laser sources allow for accurate determination of line positions,[2] and high spectral resolution (better than $1:10^7$) was demonstrated at wavelengths near 95 nm.[3] Generally these sources are less suited to be applied in direct absorption measurements, owing to their large pulse-to-pulse intensity variations, which are inherent to the nonlinear process of harmonic generation of XUV-laser radiation. For this reason tunable and narrowband XUV-laser sources are commonly used in excitation spectroscopy; signal recording then occurs by the sensitive method of $1 + 1'$ photoionization, where a first photon induces a resonant transition to a bound excited state, and a second photon of different frequency drives a nonresonant transition into the ionization continuum. In such schemes the signal strength is determined by the oscillator strength of the XUV transition, the intermediate-state lifetime, and the photoionization cross section.

The effects of instrumental bandwidth on absolute cross-section measurements were studied by Hudson and Carter.[4] They pointed out that in general the value of the peak cross section deduced from the slope of a Beer's law plot [i.e., $\ln(I/I_0)$ versus gas density N] is a lower limit to the true peak cross section, as measured absorption profiles commonly are a convolution of instrumental bandwidth and inherent linewidth. This inherent width pertains to the natural linewidth of a molecular transition and to additional effects of Doppler and/or collisional broadening. At limited instrumental resolution, peak cross sections are systematically underestimated at the top of an absorption profile, whereas cross sections measured at the wings generally overestimate the true value. These systematic effects depend on the ratio of instrumental width and inherent absorption width and become larger with increasing ratio. Stark *et al.*[5] pointed out that even in extrapolation to zero optical density (OD), measured peak cross sections will be lower limits. The measured value of the total cross section of an absorption profile will, however, always converge to the real absorption cross section in the limit of zero optical depth.[5]

The goal of our present work was to demonstrate that a tabletop XUV-laser source may be applied for direct absorption measurements by use of a novel experimental approach. The relatively large (i.e., of the order of 20%–30%) pulse-to-pulse intensity fluctuations are monitored with a diffraction grating. Comparison of the intensity in several diffracted beams results in a strongly improved applicability of our XUV source for such measurements. In a feasibility experiment we determined relative cross sections of some sharp absorption bands in CO that are relevant for the photochemical dynamics in interstellar clouds. The accuracy in the values of the absorption cross sections is increased with respect to previous data, owing to the narrow bandwidth of the employed XUV-laser source (0.28 cm^{-1} near 95 nm).

2. EXPERIMENTAL SETUP

The XUV-laser spectrometer contains a high-power pulsed laser system and a setup consisting of three differentially pumped vacuum chambers. A pulsed Nd:YAG laser (Quanta-Ray, GCR-5) is used to pump a commercial tunable dye laser (Spectra Physics, PDL-3). Tunable UV-laser light is produced by frequency doubling its output. The UV light is separated from the visible dye-laser

radiation and focused into a freely expanding jet of xenon gas in a first vacuum chamber (see Fig. 1). XUV radiation is generated via a third-harmonic process by focusing the UV beam close to the orifice of the pulsed gas valve. The phase-matching properties of this third-harmonic process ensure that a coherent XUV beam is generated in the forward direction, overlapping the intense fundamental ultraviolet beam.[6] Variations in dye-laser intensity and in xenon gas density result in pulse-to-pulse fluctuations in the XUV-light intensity of 20%–30%. The bandwidth of the generated XUV-laser radiation is determined by the bandwidth of the dye laser (0.08 cm^{-1}), leading to a bandwidth of 0.28(3) cm^{-1} at 95 nm. A further decrease of the XUV linewidth to 0.01 cm^{-1} is possible by implementing pulsed amplification of cw laser radiation.[2,3,7] However, the application of such a system to integrated band cross-section measurements is difficult, as it requires large continuous wavelength scans to record a full rotational molecular band. Therefore in the present experiment the XUV source based on an easily tunable, commercial dye-laser system was used, resulting in the 0.28-cm^{-1} XUV bandwidth. This represents a significant improvement over the widths achieved in spectroscopic studies performed at synchrotrons, where grating resolution is a limiting factor.

XUV- and UV-laser light were spatially separated in a home-built vacuum monochromator, including a commercially available concave grating (Milton-Roy; 1200 grooves/mm; blaze angle 2.8°; radius of curvature R = 1 m) used in a Seya–Namioka configuration. The absolute XUV intensity before diffraction at the grating was measured by integrating the photoelectric current from a gold-plated surface.[8] At incident UV energies of 40 mJ/pulse, XUV yields of 3.3 nJ/pulse (or 1.7

$\times$ 10^9 photons/pulse) were measured at a wavelength of 95.4 nm.[9] For the absorption measurements described below, electron multipliers with higher sensitivities were used.

To avoid surface damage of the grating by the incident intense UV-laser light, it is placed at a distance of 1 m from the tripling focus. The UV intensity on the grating is then reduced to <1 MW/cm^2 (i.e., under typical conditions of UV energies <40 mJ with a pulse duration of 5 ns; UV beam diameter of 32 mm at the grating), which is below the damage threshold. The ruled area of the grating (56 mm × 96 mm) is sufficiently large to ensure diffraction of the entire UV spot. Ultraviolet-induced photodissociation of background molecules (from diffusion pump oil) on the grating surface may degrade its reflectivity. Therefore a cold finger at liquid N_2 temperature is mounted close to the heated (~40 °C) grating, ensuring a constant grating reflectivity in time.

3. NOISE REDUCTION IN DIRECT XUV-ABSORPTION MEASUREMENTS

The nonlinear process of generation of XUV radiation results in pulse-to-pulse fluctuations in the intensity as large as 20%–30%, which severely limits the usefulness of the source for direct absorption measurements. Long averaging times are required to overcome these large statistical fluctuations, but are only of limited practical use.

From theory[6] it follows that XUV intensity I_{XUV} and UV intensity I_{UV} are related by a third-power law:

$$I_{\mathrm{XUV}} \propto n^2 |\chi^{(3)}|^2 F(\Delta k, n) I_{\mathrm{UV}}^3, \qquad (1)$$

where n is the density of the medium, $\chi^{(3)}$ is the third-order nonlinear susceptibility, and $F(\Delta k, n)$ is the phase-matching function depending on the phase-mismatch Δk between k vectors of the incident UV and generated XUV beams. However, a simultaneous measurement of UV and XUV intensity did not show a correlation. This is attributed to the intricate dependence of I_{XUV} on the density and the inhomogenities in both the laser-beam profile and the gas jet. Moreover, saturation effects reduce the correlation. Thus in practice the influence of pulse fluctuations of the XUV laser could not be eliminated by monitoring UV intensity. With the use of an XUV beam splitter the sensitivity in direct absorption measurements may be increased as well. Conventional beam splitters based on mirror coatings are not available. Alternatively, a beam splitter based on spatially splitting the beam into two distinct parts, i.e., a left and a right half of the XUV beam, was tried, with a separate detector for each part of the beam. Dividing the signals from both detectors resulted in a factor of 2.5 improvement in the signal-to-noise ratio with respect to a measurement in a single channel. The transverse coherence in the XUV beams is obviously insufficient to yield significant improvement in absorption measurements.

Encouraging results were obtained with the vacuum monochromator as a beam splitter. In the far field of the grating the overlapping intense UV beam and the XUV-laser radiation are spatially separated, and several orders (i.e., +1st and −1st order; +2nd and −2nd...) of diffracted XUV beams are observed. By a simultaneous measure-
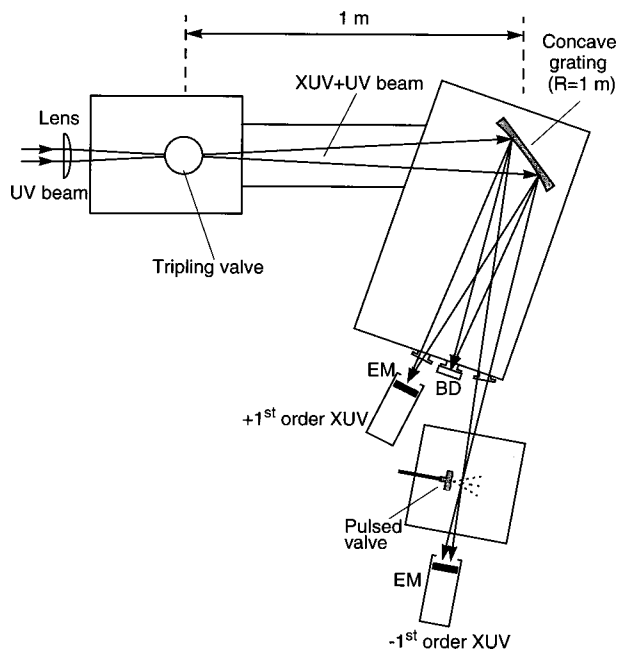

Fig. 1. Top view of the setup for direct absorption measurements. The +1st-order diffracted XUV beam is used to monitor intensity. The 1st-order diffracted XUV beam intersects a secondary pulsed molecular expansion. EM, electron multiplier; BD, beam dump for 0th-order reflected beam.

ment of the intensity in the +1st and −1st-order diffracted beams with two separate detectors (Fig. 1) one of the signals could be employed as a monitor for intensity fluctuations.

In Fig. 2 the intensities of the XUV-laser source measured in the −1st-order (upper trace) and +1st-order (middle trace) diffracted beam are plotted. For both spectra an average of ten laser pulses is displayed, corresponding to a typical 1-s averaging time (laser and pulsed valves at 10-Hz repetition rate). In both traces the intensity variations of the XUV-laser source are clearly visible, with a relative noise figure of $\sigma = \Delta I/I = 0.064$. A good correlation in the intensity fluctuations in the −1st- and +1st-order diffracted XUV beam is observed. This is also clear from the lower trace of Fig. 2, which shows the ratio of +1st- and −1st-order intensities with σ as low as 0.0068. The sensitivity of the XUV-laser source for direct absorption measurements clearly increases by an order of magnitude, as is illustrated in Fig. 3. Here, as an example, an absorption spectrum of the $c_4'\ {}^1\Sigma_u^+-X^1\Sigma_g^+(0,0)$ band of N_2 at 95.9 nm, measured with the setup of Fig. 1, is uncovered from one of the signal channels. Not only are the baseline fluctuations reduced by an order of magnitude; also the wavelength-dependent XUV yield, giving rise to a dip at 95.93 nm, is compensated for.

When a weak chaotic light source is used, its noise is ultimately governed by Poissonian photon statistics. For such a source it holds that when p measurements are performed, the relative variance $\mathrm{Var}(K_m)$ in the averaged number of photons K_m in repeated measurements K_j is

$$\mathrm{Var}(K_m) = \frac{\dfrac{1}{p} \times \displaystyle\sum_{j}^{p} (K_m - K_j)^2}{K_m^2}. \qquad (2)$$

For the ratio of two independent measurements K_m and K_m', the relative variance in the ratio K_{div} is given by

$$\mathrm{Var}(K_{\mathrm{div}}) = \mathrm{Var}(K_m) + \mathrm{Var}(K_m'). \qquad (3)$$

We wish to use this feature for a statistical analysis of our data. The noise of a multimode pulsed dye laser is usually no better than that of a chaotic light source. However, a description of the XUV intensity in terms of Poisson statistics may not be applicable. Density fluctuations in the nonlinear medium (i.e., in the xenon gas pulse), as well as inhomogeneities in the laser beam, multiplied in the upconversion process, govern the pulse-to-pulse fluctuations in the XUV radiation as measured at −1st or +1st order and certainly result in non-Poissonian statistics for each separate beam. After correlation of these pulse-to-pulse fluctuations in −1st and +1st order, the residual variance may, however, be determined mainly by Poisson statistics.

Furthermore, in the experiment, large numbers of photons are detected in a time window of 5 ns, so the individual photons cannot be counted, and we have to rely on a pulse-energy measurement. Since the XUV is produced in a directional beam of low divergence, it can be entirely detected on an electron multiplier with a 2-cm-diameter cathode, as in the present case. Therefore there is no practical distinction between irradiance and
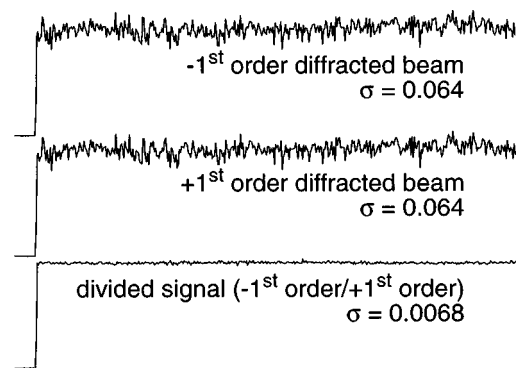

Fig. 2. Measured XUV intensity at -1st (upper trace) and +1st (middle trace) -order diffracted beams. The noise in both cases is approximateliy 6% for a 1-s (10 laser pulses) averaging time. The lower trace shows a ratio spectrum, with a noise reduction by one order of magnitude to 0.68% rms. The horizontal scale represents a time series.
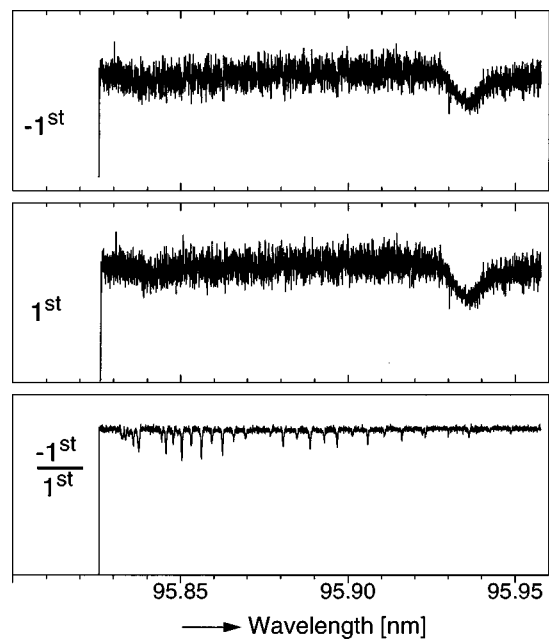

Fig. 3. Upper and middle traces show the simultaneously recorded signals from 1st- and -1st-order diffracted beams as measured with the setup of Fig. 1. The lower trace represents a ratio spectrum uncovering the $c_4'\ {}^1\Sigma_u^+ -X^1\Sigma_g^+\,(0,0)$ band of N_2, which is hidden in the signal of the -1st-order diffracted beam. Note also how the dip in the XUV intensity disappears in the correlation spectrum.

intensity. We will, in the following, term the voltage readout from a pulse-energy measurement the intensity I_m of the beam. In the measurement procedure a gain parameter g has to be considered, which relates this intensity to the number of detected photons:

$$I_m = gK_m. \qquad (4)$$

Here g represents a nondimensionless parameter, and for simplicity the quantum efficiency of the detector is included in g. We now make the assumption, based on the behavior of Poissonian photon statistics, that when gain and measured intensity of two signals are equal, i.e., $g = g'$ and $I_m = I_m'$, the relative variance in the ratio increases by a factor of 2. According to Eqs. (2)–(4) a re-

duction in XUV intensity by a known factor δ will result in a 2δ increase in residual variance, under the assumption of Poissonian statistics. Experimentally the XUV intensity was decreased in two different ways: the intensity of the fundamental UV beam I_{UV} was reduced, and, alternatively, the density n of the nonlinear medium was decreased. In both cases we found in good approximation the expected increase in the residual variance. This indicates that it is a reasonable assumption to apply Eqs. (2)–(4) to the measured intensities.

From the results shown in Fig. 2 we determine the noise figure in the ratio of two signals to be $\sigma(I_m) = 0.0068$ for an average over ten laser shots. This standard deviation, defined as $\sigma(I_m) = [\text{Var}(I_m)]^{1/2}$, leads to a relative variance of 4.6×10^{-5}, i.e., 4.6×10^{-4} per pulse. Assuming the gain and quantum efficiency of both electronmultipliers to be equal, a relative variance for a single channel, (i.e., the -1st or $+1$st-order diffracted XUV beam) of 2.3×10^{-4} (noise figure of $\sigma = \Delta I/I = 0.015$) results. From this analysis and the above assumptions for the noise behavior, with the single-channel noise figure of 0.015/pulse, the number of photons detected on one electron multiplier is 4.3×10^3 per pulse. Again, we note that the noise characteristics of the XUV intensity were not explicitly measured, nor was it proven to be Poissonian. However, the dependence of the residual variance on the XUV intensity is similar to that of a Poissonian distribution, at least in the intensity range of the present measurements.

The reflectivity of our grating for diffraction at 95.4 nm for *s*-polarized XUV light was experimentally determined at 0.71(7)% using current-measuring gold plates[9] for incident and diffracted beams at the grating. For *p*-polarized light the grating efficiency was found to be an order of magnitude less. For a typical *s*-polarized beam of 1.7×10^9 photons/pulse the number of photons diffracted by the grating is $\sim 1.2 \times 10^7$/pulse, in both -1st and $+1$st orders. A quantum efficiency for one electron multiplier of 4×10^{-4} is then deduced, which is rather low for 95-nm photons. However, degenerated electronmultipliers with photocathodes exposed to oil from a diffusion pump for an extended period of time were used in this experiment, and a low gain and quantum efficiency for XUV radiation was no surprise.

This analysis of the statistical properties of the XUV-laser source shows that the observed noise in our experiment was related to the low count rate at the electron multipliers. This indicates a possibility for improvement, to be achieved by employing detectors with higher quantum efficiencies and a grating with higher reflectivity.

4. PHOTOABSORPTION CROSS SECTIONS OF CO IN THE WAVELENGTH RANGE 95.6–97.3 NM

According to Lambert–Beer's law, the intensity I measured after absorption of light in a medium is given by

$$I = I_0 \exp(-\sigma n l), \qquad (5)$$

where I_0 is the intensity incident on the medium, σ is the absorption cross section, n is the density, and l is the ab-

sorbing path length. XUV-absorption spectroscopy in molecular jets has been demonstrated to be a useful technique for cross-section measurements.[10] Although the absorption path length is reduced to ~ 1 cm, the (partial) pressure in the molecular expansion close to the orifice of the nozzle may be quite high. A molecular column density $N = nl$ of 10^{15} cm^{-2} is readily achieved, which is sufficient to measure absorption cross sections of the order of 10^{-16} cm^2. An additional advantage of the use of free jets is that, at a distance of 10 nozzle diameters, the collision-free regime is reached.

The integrated band cross section $\sigma_{\text{vib}}(\lambda)$ of a molecule is independent of the distribution over rotational states, and is defined as

$$\sigma_{\text{vib}}(\lambda) = \frac{1}{N} \int_{\lambda_1}^{\lambda_2} \ln \frac{I_0(\lambda)}{I(\lambda)}. \qquad (6)$$

Here λ_1 and λ_2 are the boundaries determined by the spectral extension of the vibrational band (governed by the rotational temperature of the gas sample); $I(\lambda)$ is the intensity transmitted by the absorbing medium. In a molecular expansion, low rotational temperatures can be reached. Given the invariance of $\sigma_{\text{vib}}(\lambda)$, the peak cross section of transitions originating from low rotational quantum numbers will grow when the internal motions of the molecule (i.e., vibration and rotation) freeze out, thus resulting in an increased effective column density per quantum state at low rotational temperatures. The accuracy in the measured band cross section will benefit from such a low internal temperature. An additional advantage is that rotational overlap between adjacent vibrational bands is circumvented.

With the grating spectrometer described in Section 2, absorption spectra of CO in the wavelength range 95.6–97.3 nm were recorded. In Fig. 4, several examples of such spectra are reproduced. In this part of the CO spectrum, sharp (i.e., Lorentzian widths Γ approximately equal to the instrumental width of 0.28-cm^{-1} FWHM), intermediate ($\Gamma = 1$–2 cm^{-1}), and diffuse ($\Gamma > 2$ cm^{-1}) absorption profiles can be discerned. These bands were also observed by other groups,[11–13] but with lower resolution. Here we concentrate on five intermediate and sharp features: the $K^1\Sigma^+(v' = 0)$–$X^1\Sigma^+$, $W^1\Pi(v' = 1)$–$X^1\Sigma^+$, $L^1\Pi(v' = 0)$–$X^1\Sigma^+$, $L'\ {}^1\Pi(v' = 1)$–$X^1\Sigma^+$, and $W^1\Pi(v' = 0)$–$X^1\Sigma^+$ band systems (see Fig. 4).

The setup for direct absorption measurements is schematically shown in Fig. 1. The secondary nozzle, which produces a pulsed CO expansion, is placed at a distance of ~ 90 cm from the concave grating. With the concave grating used in a geometry, close to a Seya–Namioka configuration (angles of incidence and reflection are 68°), the image formed by a spherical grating will be astigmatic, and two separate line-foci are observed. At a distance of 90 cm a symmetrically shaped XUV image of 10-mm diameter is formed in the -1st-order diffracted beam.[9,14]

As the integrated band cross section is invariant for rotational temperature, a comparison of the cross section determined in a static gas (with known column density) with the cross section measured at jet temperature gives a direct measure of the column density in the jet.[10]
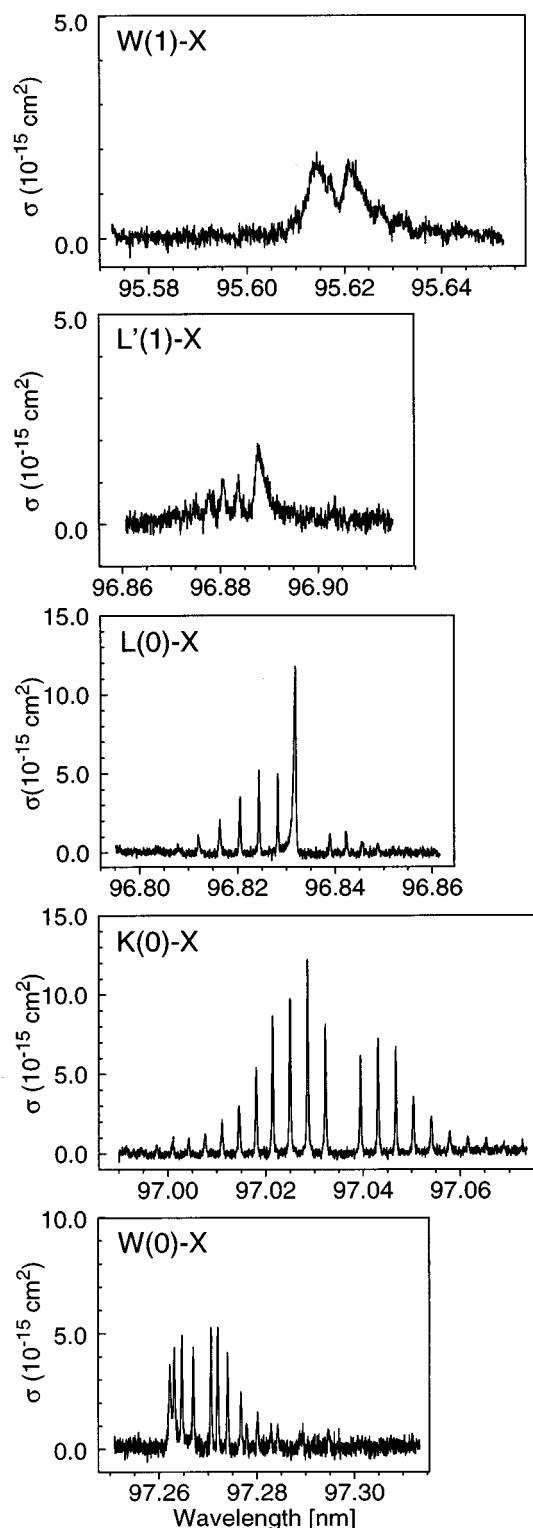
Fig. 4.   Measured photoabsorption spectra for five bands of CO in the wavelength range 95.6–97.3 nm.

the reported cross section of (2.23 ± 0.44) $\times$ 10^{-17} cm^2 nm it follows that column densities in our experiment were of the order of 10^{14} cm^{-2}.

All five bands were measured at three or four different column densities. The final value for the cross section is calculated as an average of the results obtained for these different column densities. Integrated band cross sections relative to the $K(0)$–X system are collected in Table 1. The true optical depth (OD), that is, the OD corrected for the instrumental linewidth of 0.28 cm^{-1}, never exceeded 0.8, and most bands have been measured at OD < 0.4. At the low rotational temperatures of approximately 50 K in our expansion, the observed vibrational bands show no rotational overlap. For the $L(0)$–X and $K(0)$–X bands a series of measurements was recorded at a higher rotational temperature ($\sim$100 K) in order to reduce the OD on the most intense lines [such as the Q branch in the $L(0)$–X band]. Relative peak cross sections are displayed in Fig. 4 for the five bands measured between 95.7 and 97.3 nm. A comparison with the highest resolution absorption data previously obtained[11] shows higher peak cross sections in the present data. The resolution $\lambda/\Delta\lambda$ achieved in our experiment at 96 nm is $\sim$370 000 compared with a resolution of 175 000 in the experiments of Stark *et al.*[11]

The background pressure of CO molecules in our experiment was monitored during a series of six consecutive scans [i.e., $W(1)$–X, $L(0)$–X, $L'(1)$–X, $K(0)$–X, $W(0)$–X bands, and again the $W(1)$–X band] and proved to be a reliable experimental parameter to keep column density and internal state distribution at constant values. We therefore take relative band cross sections at a given column density to be accurate within 15%. The averaged relative cross sections given in Table 1 are estimated to have an error margin of 10%.

Table 1 shows a good agreement between our relative band cross sections and those measured by Stark *et al.*[11] Comparison with room-temperature spectra measured by Eidelsberg and Rostas[12] and Stark *et al.*[5] show larger deviations from the present data, especially for bands that overlap with high rotational lines of adjacent vibrational transitions [e.g., $L(0)$–X and $K(0)$–X]. This clearly demonstrates the beneficial effect of the low rotational temperatures in our molecular expansion.

Stark *et al.*[11] have shown that instrumental bandwidth corrections of their spectrometer for the $K(0)$–X band were less than 4%, and cross sections determined from both room- and jet-temperature spectra agree very well. For this reason we selected the cross section of the $K(0)$–X band as measured by Stark *et al.*[11] to calibrate the column density in our molecular expansion. From

Table 1.   Measured Integrated Band Cross Sections of CO in the Wavelength Range 95.7–97.3 nm Relative to the $K(0)$–X Band Cross Section: $\sigma_{K(0)} = (2.23 \pm 0.44) \times 10^{-17}$ cm^2 nm^{11} [a]

Band	Integration Limits	This work	Ref. 11	Ref. 12	Ref. 5
$K(0)$–X	$\lambda = 96.98$–97.08 nm	1	1	0.78	0.50
$W(1)$–X	$\lambda = 95.60$–95.65 nm	0.66		0.49	0.54
$L(0)$–X	$\lambda = 96.81$–96.85 nm	0.49	0.43	0.29	>0.33
$L'(1)$–X	$\lambda = 96.87$–96.90 nm	0.29	0.27	0.46	0.32
$W(0)$–X	$\lambda = 97.26$–97.30 nm	0.52	0.48	0.45	0.48

[a] Comparisons with previous measurements, which yielded absolute cross sections, are given in the last three columns. For convenience of comparison the data of Refs. 12 and 5 were also scaled to $\sigma_{K(0)}$ of Ref. 11.

5. CONCLUSIONS

A novel experimental technique was developed to calibrate and monitor the intensity variations of an XUV-laser source. An XUV vacuum monochromator was combined with an XUV-laser source to disperse the harmonically generated XUV radiation into several distinct exit ports. A simultaneous measurement of XUV intensity at the exit ports for -1st and $+1$st-order diffracted beams gave possibilities to compensate large intensity fluctuations of the source, and a noise figure of 0.68% rms was obtained at a typical averaging time of 1 s. Because of low quantum efficiency of the detectors and a low grating reflectivity, the present absorption measurements were performed at count rates of 4300 photons/s. This number can be compared with the number of photons measured at the exit slit of the high-resolution spectrometer 6VOPE at the synchrotron facility Photon Factory in Tsukuba, Japan.[1]   There, a count rate of $\sim$600 photons/s for jet-absorption measurements and $\sim$6000 photons/s for room-temperature measurements have been reported.[11]   It was demonstrated that the sensitivity for direct absorption measurements in our case was related to the low number of photons detected. Implementation of a detector with increased quantum efficiency and of a grating with a reflectivity higher than 0.71% is likely to result in a lower noise figure and thus in a higher sensitivity for direct absorption spectroscopy. With the noise-calibrated source, high-quality absorption data of CO in the range 95.6–97.3 nm were obtained. These measurements were performed at the highest resolving power demonstrated in direct absorption, and resulted in an accurate determination of (relative) absorption cross sections of CO.

ACKNOWLEDGMENTS

REFERENCES

1. K. Ito, K. Maeda, Y. Murioka, and T. Namioka, "Performance of the 6VOPE high resolution VUV spectroscopic facility in the photoelectric detection mode," Appl. Opt. **28**, 1813–1817 (1989).
2. K. S. E. Eikema, W. Ubachs, W. Vassen, and W. Hogervorst, "Lamb shift measurements in the $1\ {}^1S$ ground state of helium," Phys. Rev. A **55**, 1866–1884 (1997).
3. W. Ubachs, K. S. E. Eikema, W. Hogervorst, and P. C. Cacciani, "Narrow-band tunable extreme-ultraviolet laser source for lifetime measurements and precision spectroscopy," J. Opt. Soc. Am. B **14**, 2469–2476 (1997).
4. R. D. Hudson and V. L. Carter, "Bandwidth dependence of measured UV absorption cross sections of argon," J. Opt. Soc. Am. **58**, 227–232 (1968).
5. G. Stark, K. Yoshino, P. L. Smith, K. Ito, and W. H. Parkinson, "High-resolution absorption cross sections of carbon monoxide bands at 295 K between 91.7 and 100.4 nm," Astrophys. J. **369**, 574–580 (1991).
6. R. W. Boyd, *Nonlinear Optics* (Academic, New York, 1992).
7. E. Cromwell, T. Trickl, Y. T. Lee, and A. H. Kung, "Ultranarrow bandwith VUV–XUV laser system," Rev. Sci. Instrum. **60**, 2888–2892 (1989).
8. R. B. Cairns and J. A. R. Samson, "Metal photocathodes as secondary standards for absolute intensity measurements in the vacuum ultraviolet," J. Opt. Soc. Am. **56**, 1568–1573 (1966).
9. P. C. Hinnen, "XUV-laser spectroscopy of H_2 and the mystery of the diffuse interstellar bands," Ph.D. dissertation (Vrije Universiteit, Amsterdam, 1997).
10. K. P. Huber and Ch. Jungen, "High-resolution jet absorption study of nitrogen near 800 Å," J. Chem. Phys. **92**, 850–861 (1989).
11. G. Stark, K. Yoshino, P. L. Smith, J. R. Esmond, K. Ito, and M. H. Stevens, "High-resolution absorption cross section measurements of carbon monoxide at 20 K between 96.7 and 98.8 nm," Astrophys. J. **410**, 837–842 (1993).
12. M. Eidelsberg and F. Rostas, "Spectroscopic, absorption and photodissociation data for CO and isotopic species between 91 and 115 nm," Astron. Astrophys. **235**, 472 (1990).
13. K. P. Huber, G. Stark, and K. Ito, "Rotational structure in the Hopfield series of N_2," J. Chem. Phys. **98**, 4471–4477 (1992).
14. H. G. Beutler, "The theory of the concave grating," J. Opt. Soc. Am. **35**, 311–350 (1945).